ACS NANOSCIENCE Au
AN OPEN ACCESS JOURNAL OF THE AMERICAN CHEMICAL SOCIETY

pubs.acs.org/nanoau Article

Influence of Cell Type on the Efficacy of Plasmonic Photothermal Therapy

Helena Villuendas, Clara Vilches,* and Romain Quidant*

Cite This: *ACS Nanosci. Au* 2022, 2, 494–502 Read Online

ACCESS | Metrics & More | Article Recommendations | Supporting Information

ABSTRACT: In plasmonic photothermal therapy (PPTT), illuminated gold nanoparticles are locally heated to produce selective damage in cells. While PPTT is expected to strongly depend on the cell line, available data are sparse and critical parameters remain unclear. To elucidate this pivotal aspect, we present a systematic study of diseased and nondiseased cells from different tissues to evaluate cytotoxicity, uptake of gold nanorods (AuNRs), and viability after PPTT. We identified differences in uptake and toxicity between cell types, linking AuNR concentrations to toxicity. Furthermore, the cell death mechanism is shown to depend on the intensity of the irradiated light and hence the temperature increase. Importantly, the data also underline the need to monitor cell death at different time points. Our work contributes to the definition of systematic protocols with appropriate controls to fully comprehend the effects of PPTT and build meaningful and reproducible data sets, key to translate PPTT to clinical settings.

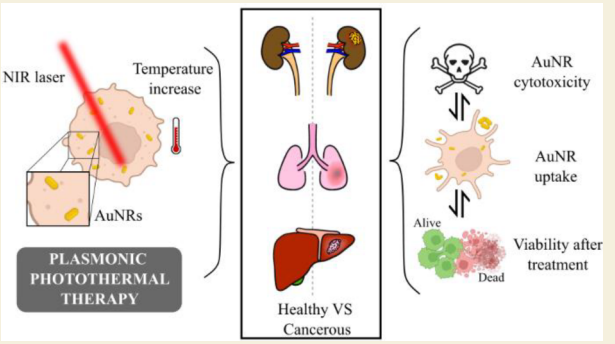

KEYWORDS: *Hyperthermia, Plasmonic photothermal therapy, Viability, Systematic, In vitro*

Hyperthermia is defined as a moderate increase of temperature above physiological values (>37 °C) for defined periods of time.[1,2] Increases of temperature have been used as a treatment for pathological conditions in different medical specialties,[3] specifically in oncology, where hyperthermia has great potential as a standalone therapy or as an adjuvant to current therapies.[2−5]

However, in conventional hyperthermia, there is a lack of specificity and temperature control that can cause significant collateral damage.[6,7] In more recent years, nanomedicine has explored new approaches to therapeutic hyperthermia, like plasmonic photothermal therapy (PPTT), which aims to locally control the temperature increment in a specific and precise way.[8−10]

PPTT exploits the enhanced optical absorption of noble metal nanoparticles, at their localized surface plasmon resonance (LSPR), to treat malignant cells upon exogenous illumination.[11,12] Among the different types of plasmonic particles, gold nanorods (AuNRs) combine efficient light-to-heat conversion with precise tuning, with their main longitudinal LSPR in the NIR biological optical window, where tissues have minimum absorption.[13−15] Moreover, the biocompatibility and low cytotoxicity of AuNRs, easy functionalization and customization, high light absorption efficacy, colloidal stability, and scalable synthesis make them stand out as photothermal agents for PPTT.[15−17]

PPTT involves a broad parameter space that complicates data comparison from different studies and groups. Nanomaterial type, cytotoxicity, uptake, and efficient light-to-heat conversion[8,18−20] need to be considered to assess the safety and efficacy of nanoparticles for PPTT, but the use of different nanoparticles, cell types, and methods to study viability between groups hinders the transition of PPTT toward clinical applications.[18] Systematic experimentation of *in vitro* PPTT is essential for effective data comparison and development of PPTT.

Studying PPTT in an *in vitro* setting allows for more accurate control of the chemical and physical environment, including more efficient exploration of the parameter space. In addition to minimizing the number of animals used and allowing research at a reduced cost, most diseases have *in vitro* models and more tools are available to study the molecular mechanisms triggered by the therapy.

Several studies have explored the roles that nanoparticle morphology, functionalization, and method of incubation play in cytotoxicity and uptake in different *in vitro* models.[17,21−27] Recently, Zhao *et al.* studied the differential toxicity mechanisms of spherical gold nanoparticles (AuNSs), compar-

Received: May 17, 2022
Revised: July 8, 2022
Accepted: July 13, 2022
Published: July 27, 2022

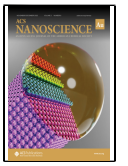

https://doi.org/10.1021/acsnanoscienceau.2c00023
ACS Nanosci. Au 2022, 2, 494–502

ing their effects in two different types of renal cells. Significant toxicity was found for renal cancer cells independent of the concentration, nanoparticle size, and incubation time, whereas normal renal cells presented high levels of autophagy, which seemed to protect them from damage.[22] In another work, Xia *et al.* studied the cytotoxicity and uptake of AuNS in hepatic cell lines. Data showed a higher susceptibility for the normal hepatic cell line L02 compared to cancer HepG2 cells. At the same time, they reported different uptake capacities of AuNSs between normal and cancer hepatic cells but did not positively correlate it to cytotoxicity.[23] This manifests the need to use controls and off-target cell lines to completely understand the effects of PPTT.

Employing the appropriate controls when studying nanoparticle toxicity is important for the compatibility and efficacy of the therapy. In clinical applications, intravenous administration of nanoparticles is the standard route of administration, and it involves a systemic biodistribution of the nanoparticle load and uptake by off-target cell types. Eventually, the toxicity of the nanoentities toward healthy tissues is a crucial aspect to determine the safety of nanoparticles.

In parallel to the effects of AuNPs, effects of laser irradiation should be studied in the presence or absence of nanoparticles.[10,27−31] Ideally, a synergistic effect arises from the combination of AuNPs and laser irradiation, generating an increase of temperature. Laser settings (power density, beam diameter, time of irradiation) must be planned to increase local temperature, avoiding damage to cells without nanoparticles. Almada *et al.* showed that irradiation for 5 min at the higher laser power (2 W) decreased cellular viability even in the absence of AuNRs, whereas cells irradiated with AuNRs saw their viability impaired with lower laser powers such as 1 W.[27] Furthermore, Zhang *et al.* showed how colocalization of AuNRs with laser irradiation increases temperature locally and impairs cellular viability, highlighting how different temperatures produce different cell death types.[28]

In this paper, we report the effects of PPTT, from the cytotoxicity of the nanomaterial to the outcomes of hyperthermia, in cancerous and noncancerous cell lines of three different organs. Epithelial kidney, lung, and liver cell lines were used to determine differences in the efficacy of PPTT in cancer cell lines. These organs are possible targets for PPTT and have a role in nanomedicine biodistribution and clearance. Noncancerous cell lines were used as controls to determine the safety of the nanoparticles as well as to evaluate the consequences of collateral uptake and illumination. Cytotoxicity was assessed by means of mitochondrial activity, whereas uptake was quantified with two-photon microscopy. PPTT was evaluated at two different time points by studying the mitochondrial activity and membrane integrity. With this systematic study, we demonstrate the safety and efficacy of PPTT in an *in vitro* setup, highlighting the importance of creating reliable, reproducible, and meaningful data sets that are comparable between studies and groups that use different types of nanoparticles or laser irradiation.

RESULTS AND DISCUSSION

In Vitro Quantification of AuNR-PEG Uptake

Uptake is dependent on the type and surface charge of the nanoparticles used,[32] but the functionalization and cell type will also have a role in the process of internalization. Quantification of AuNR-PEG in different cell types and tissues was performed to detect uptake performance differences. Uptake (AuNR-PEG/cell) was measured over a fixed incubation time and increasing AuNR concentrations. Cancer cell lines had a statistically higher uptake per cell compared to the same tissue noncancerous cells (Figure 1). It has been

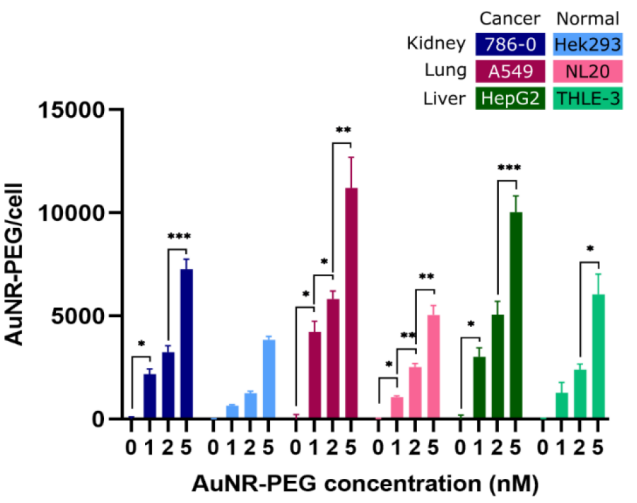

Figure 1. Uptake of AuNR-PEG as a function of concentration for different cell lines. *$p < 0.05$, error bars represent SEM ($n = 3–6$). No statistical differences were observed between all conditions for Hek293 and 0−1 nM for THLE-3.

described that cancer cells more readily incorporated AuNPs with higher concentrations compared to healthy cells,[23] but we note that for all cell types there was an increase in uptake with concentration. The lower uptake of normal cell lines is consistent with the incubation of AuNRs in cell culture medium that contained 5−10% FBS, compared to FBS-free medium in cancer cell lines. The presence of protein containing medium during AuNR incubation can decrease the surface reactivity and uptake of AuNPs by cells.[17,25]

The 786-0 cell line had a statistically lower uptake than A549 and HepG2. Hek293 also had lower uptake than the other noncancerous cell lines studied, showing a trend in kidney cells with a lower uptake of AuNR-PEG *in vitro* compared with lung or liver cell lines under the same conditions.

Among the studied concentrations, the highest uptake observed was obtained with a AuNR-PEG concentration of 5 nM (Figure 1), but for nontoxic concentrations of gold (≤2 nM, Figure 2A) incubations with 2 nM meant a higher uptake for all studied cell lines without compromising cellular viability under 70% (Figure S2).[33] Selecting the correct concentration for incubation will determine the cytotoxicity of AuNR-PEG and impact its performance during irradiation, as temperature generation will be influenced by the presence of AuNR-PEG in cells.

The assessment of cellular uptake among different tissues is important because, for *in vivo* PPTT, nanoparticles are preferentially administered via the bloodstream, exposing both the target (tumoral cells) and surrounding tissues to nanoparticles. Selecting appropriate cell lines for the study of PPTT will be crucial for its development. We report on lung cell lines as an example of a target tissue that is extremely exposed to external aggressions and one of the most diagnosed cancers in the world.[34] We also studied liver and kidney

https://doi.org/10.1021/acsnanoscienceau.2c00023
ACS Nanosci. Au 2022, 2, 494−502

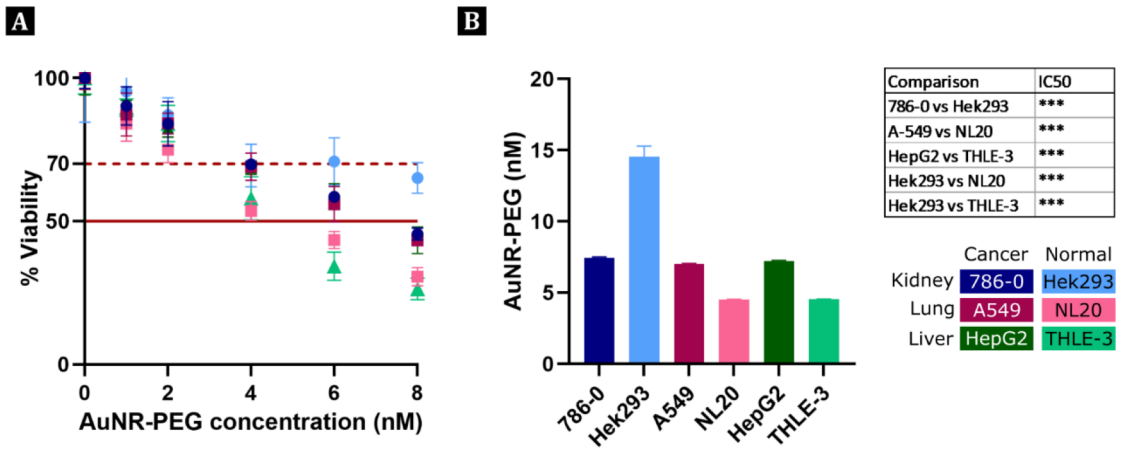

Figure 2. Effect of AuNR-PEG concentration on cellular viability. (A) Viability of cell lines for all studied concentrations shown as percent of controls (0 nM). (B) IC_{50} of cell lines. ***$p < 0.001$. Error bars represent SEM ($n = 4$).

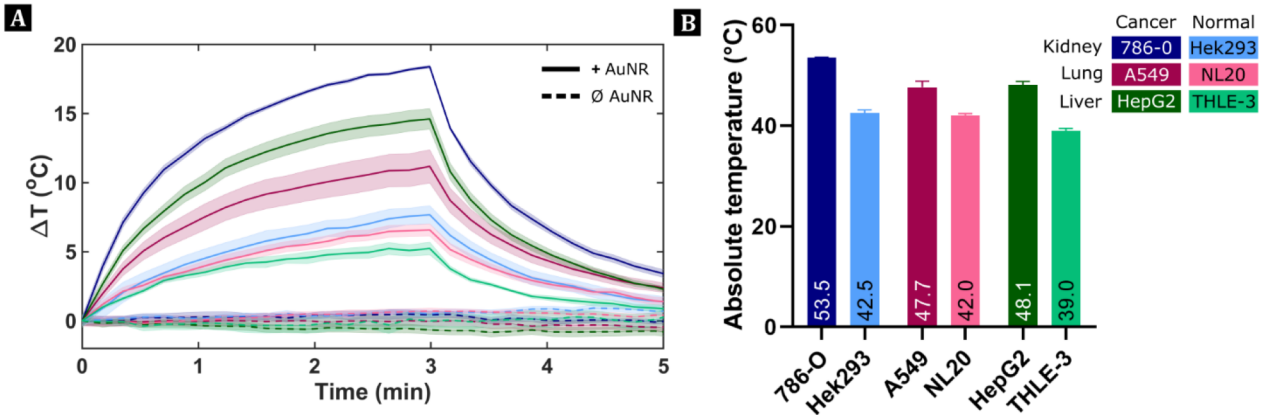

Figure 3. Temperature dynamics in +AuNR-PEG and ØAuNR cells upon irradiation. (A) Increase in temperature as a function of time for cell lines irradiated 3 min with an 808 nm laser light at 3 W/cm^2. Continuous line indicates cells with AuNR-PEG (+AuNR-PEG) and dotted line cells without AuNR-PEG (ØAuNR-PEG). Shaded line represents the SEM. (B) Averaged absolute increases of temperature of cells + AuNR-PEG.

derived cells as key tissues that, as part of the mononuclear phagocytic system and renal clearance, respectively, will be responsible for a high sequestration of nanoparticles after intravenous administration.[35]

Overall, under the same conditions, cancerous and noncancerous epithelial cell lines have different uptake capabilities, which is also seen between different tissues, compromising the efficacy of PPTT and highlighting the importance of studying more than one cell type to determine the uptake of nanoparticles.

In Vitro Determination of AuNR-PEG Toxicity

To assess nanomaterial cytotoxicity, thiazolyl blue tetrazolium bromide (MTT) was used to determine the toxic potential of AuNR-PEG in cancerous and noncancerous cell lines of three different tissues. MTT measures the metabolic activity of cells, directly dependent on mitochondrial respiration, which is interpreted as a measure of cellular viability. Results showed how exposure to low AuNR-PEG concentrations (≤2 nM) equivalent to less than 104 μg/mL of gold was not toxic to cells, whereas increases in concentration decreased the survival rate to less than 70% after 24 h of exposure. As stated by Kim *et al.*, and according to the International Organisation for Standardisation (ISO), if the cell survival rate is less than 70%, a substance is defined as cytotoxic. In this particular case, cytotoxicity is both concentration and cell type dependent.[33]

The impact of high gold concentrations was more pronounced in noncancerous NL20 and THLE-3 cell lines, while Hek293 showed high resistance to various gold concentrations (Figure 2), indicating dissimilarities between healthy cells from different tissues. Between cancerous cell lines, no statistical relevant differences were found at any of the concentrations evaluated. Regarding differences between the same tissue cell types, statistical differences were observed only at ≥4 nM concentrations. Noncancer cell lines had statistically lower survival rates than cancerous cell lines; however, Hek293 had statistically higher viability compared with the 786-0 cancer kidney cell line.

To determine sensitivity of the different cell lines to AuNR-PEG, IC_{50} values were calculated (Figure 2B). The concentration at which the survival rate dropped to 50% was around 7 nM for all three cancer cell lines, confirming they have a similar response to the toxic potential of AuNR-PEG in the absence of light. Normal NL20 and THLE-3 cell lines had lower IC_{50} values around 5 nM, showing the least resistance to higher gold concentrations. On the other hand, Hek293 had an IC_{50} of almost 15 nM, showing high resistance to AuNR-PEG.

Remarkably, no differences between the two lowest concentrations used (52 and 104 μg/mL, 1−2 nM) were found for any of the cell lines. This is relevant as cell survival is elevated with the highest nontoxic concentration of 2 nM

https://doi.org/10.1021/acsnanoscienceau.2c00023
ACS Nanosci. Au 2022, 2, 494−502

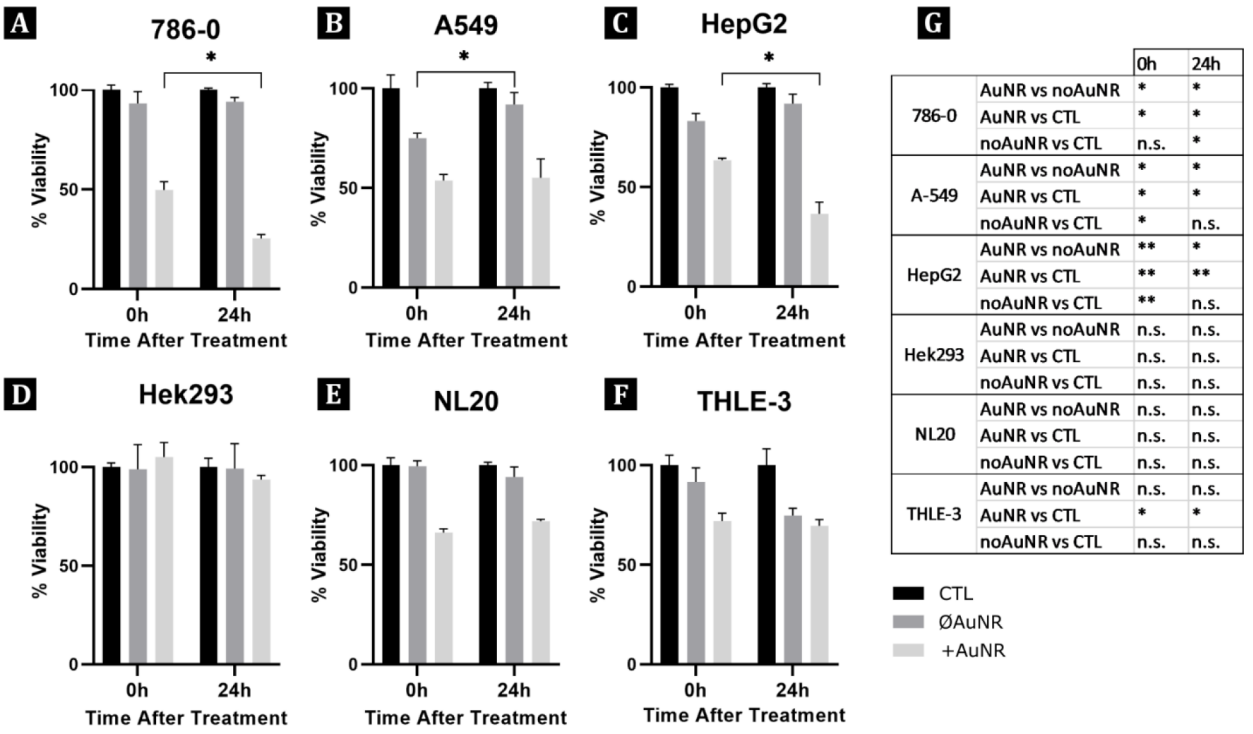

		0h	24h
786-0	AuNR vs noAuNR	*	*
	AuNR vs CTL	*	*
	noAuNR vs CTL	n.s.	*
A-549	AuNR vs noAuNR	*	*
	AuNR vs CTL	*	*
	noAuNR vs CTL	*	n.s.
HepG2	AuNR vs noAuNR	**	*
	AuNR vs CTL	**	**
	noAuNR vs CTL	**	n.s.
Hek293	AuNR vs noAuNR	n.s.	n.s.
	AuNR vs CTL	n.s.	n.s.
	noAuNR vs CTL	n.s.	n.s.
NL20	AuNR vs noAuNR	n.s.	n.s.
	AuNR vs CTL	n.s.	n.s.
	noAuNR vs CTL	n.s.	n.s.
THLE-3	AuNR vs noAuNR	n.s.	n.s.
	AuNR vs CTL	*	*
	noAuNR vs CTL	n.s.	n.s.

Figure 4. Cellular viability (%) after treatment assessed with MTT assay. (A–F) Viability at 0 and 24 h after irradiation in control (CTL) and in cells irradiated with AuNR-PEG (+AuNR-PEG) and without (øAuNR-PEG). (G) Statistical comparison for each cell line at different time points between conditions from panels (A) to (F). Differences between 0 and 24 h are shown in the graphs. Statistical comparisons were made using Tukey/Wilcox post hoc tests. *$p \leq 0.05$; **$p \leq 0.01$; ***$p \leq 0.001$; ns, not significant.

(Figure S3), and at the same time more uptake is observed when studying internalization for all cell lines after the same incubation time. For this reason, maintaining a constant incubation of AuNR of 2 nM (104 μg/mL gold) and 24 h was ideal to further study the effects of PPTT in different cell types at different times after treatment.

Resistance to different doses or exposure times will be cell type dependent, but most nanotoxicology studies focus their efforts on targeting cells, disregarding the impact on nontarget cells.[36,37] *In vitro* PPTT data focuses mostly on the cellular response of cancer cells, but the differences in uptake shown above confirm the need to study cytotoxicity in off-target tissues, as the mechanisms triggered after contact with the nanomaterial may differ between cell types. Zhao *et al.* determined that the noncancerous cell line HK-2 is more resistant than the 786-0 cancer kidney cell line to spherical AuNPs of different sizes at increasing concentration, as the autophagy mechanism employed to incorporate the nanoparticles seemed to protect them from harm,[22] and their results agree with our findings that the cancer 786-0 cell line is more susceptible to high concentrations of AuNRs than normal cells. Moreover, the increased susceptibility of noncancerous hepatic L02 cells compared to HepG2 cells with spherical AuNPs[23] is also in good agreement with our results showing lower IC_{50} values for normal THLE-3 cells compared with cancer HepG2 hepatic cells.

Photothermal Irradiation

The temperature of all six cell lines irradiated at a fixed power density (3 W/cm^2) and irradiation time (3 min) are shown in Figure 3. The increase in temperature followed a quasi-exponential increase until it reached a plateau for cell lines with AuNR-PEG. After 3 min, when laser irradiation stopped, a rapid diffusion of heat to the air and medium was observed, which translated to a drop in temperature.

Differences in final temperatures achieved were detected among cell lines (Figure 3B). Cancer cell lines (786-0, A549, and HepG2) experienced larger increases in temperature compared to noncancerous ones (Hek293, NL20, and THLE-3). For noncancerous cell lines, PPTT treatment resulted in maximum temperatures around 42 °C, while for cancer cell lines maximum temperatures were greater than 47 °C. In the case of the 786-0 cell line, the increase of temperature (over 53 °C) was statistically significant compared to that for A549 and HepG2 cells.

For cells irradiated without AuNR-PEG (Figure 3), no statistically relevant increase of temperature was detected. Namely, an average increase of 0.28 °C, up to a maximum temperature of 34.58 °C, was observed for all six cell lines studied (Figure S4).

This data allows us to observe the dynamics of light-to-heat conversion inside cells by AuNR-PEG, emphasizing the importance of recording the temperature of the different cell lines being irradiated. In all cases, cancer cell lines achieved statistically higher temperatures than noncancerous cell lines in the presence of AuNR-PEGs. At the same time, we confirm that increases of temperature are caused by the interaction of AuNR-PEGs with laser light, as cells irradiated in the absence of nanoparticles did not experience light-to-heat conversion. The addition of a third dimension during irradiation has two main consequences: collective thermal effects increase while heat dissipation with the surrounding area is reduced. Eventually both effects contribute to the increase in temperature experienced by the cells.[38] Differences in the increase of temperature can be the result of the different amount of

https://doi.org/10.1021/acsnanoscienceau.2c00023
ACS Nanosci. Au 2022, 2, 494–502

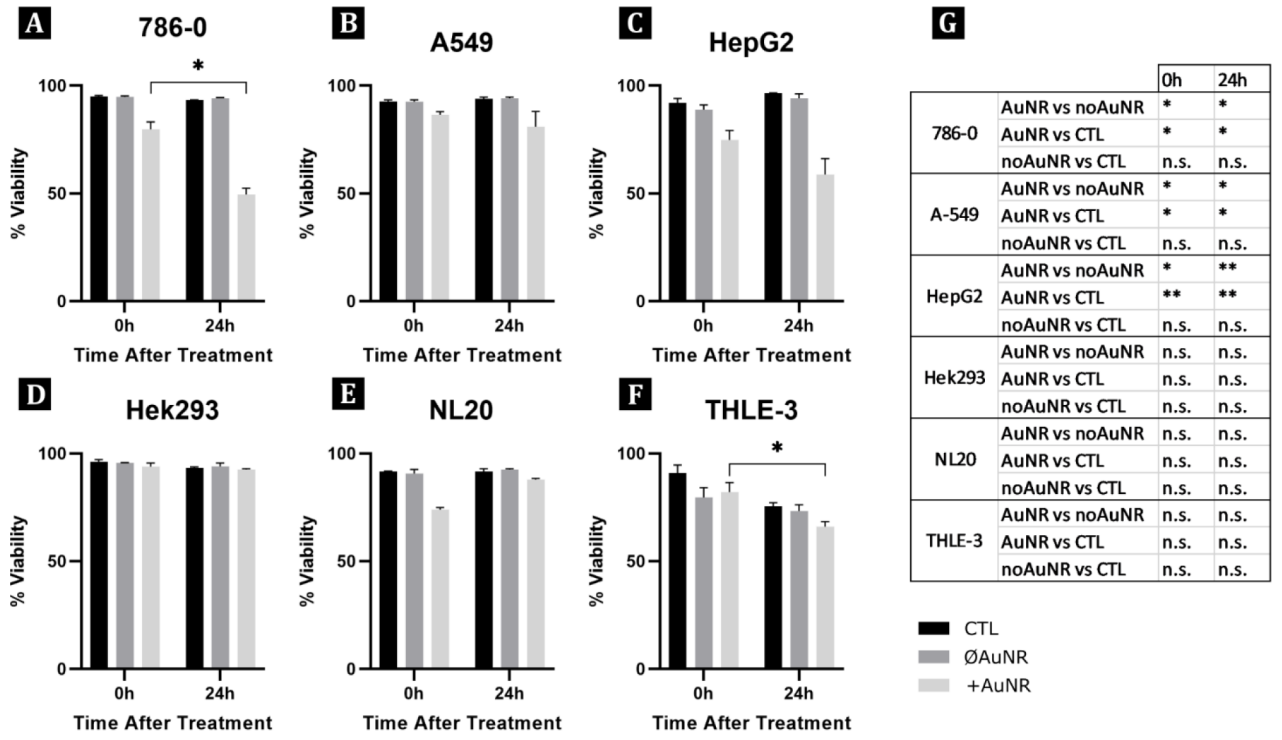

G

		0h	24h
786-0	AuNR vs noAuNR	*	*
	AuNR vs CTL	*	*
	noAuNR vs CTL	n.s.	n.s.
A-549	AuNR vs noAuNR	*	*
	AuNR vs CTL	*	*
	noAuNR vs CTL	n.s.	n.s.
HepG2	AuNR vs noAuNR	*	**
	AuNR vs CTL	**	**
	noAuNR vs CTL	n.s.	n.s.
Hek293	AuNR vs noAuNR	n.s.	n.s.
	AuNR vs CTL	n.s.	n.s.
	noAuNR vs CTL	n.s.	n.s.
NL20	AuNR vs noAuNR	n.s.	n.s.
	AuNR vs CTL	n.s.	n.s.
	noAuNR vs CTL	n.s.	n.s.
THLE-3	AuNR vs noAuNR	n.s.	n.s.
	AuNR vs CTL	n.s.	n.s.
	noAuNR vs CTL	n.s.	n.s.

Figure 5. Cellular viability (%) after treatment assessed with Trypan Blue staining. (A–F) Viability at 0 and 24 h after irradiation in control (CTL) and in cells irradiated with AuNR-PEG (+AuNR-PEG) and without (øAuNR-PEG). (G) Statistical comparison for each cell line at different time points between conditions from panels (A) to (F). Differences between 0 and 24 h are shown in the graphs. Statistical comparisons were made using Tukey/Wilcox post hoc tests. *$p \leq 0.05$; **$p \leq 0.01$; ***$p \leq 0.001$; ns, not significant.

internalized nanoparticles and the total amount of gold in the suspension[21] which will elicit different responses from the cells.

Viability after irradiation was assessed at two different time points after treatment (0 and 24 h) with two complementary methods (MTT assay and Trypan Blue staining), shown in Figures 4 and 5, respectively. The MTT assay showed mitochondrial activity as a reporter of cellular viability, whereas Trypan Blue staining reported on the loss of membrane integrity, labeling cells as nonviable. The assessment of multiple end points with more than one method[39] allows one to identify the molecular pathways activated by PPTT in both target and nontarget tissues.

For the MTT assays, cells without AuNR-PEG and not irradiated were used as a viability control (CTL). Irradiated cells without AuNR-PEG (labeled as øAuNR) maintained their viability over 70%, immediately and 24 h after treatment (Figure 4A–F). Following the cytotoxicity evaluation of AuNR, we established >70% viability of cell lines as a criterion to determine if laser light conditions were toxic to cell lines. Altogether, we show that the laser parameters used (cw 808 nm, 3 W/cm^2, 3 min irradiation) can be considered nontoxic for all six cell lines studied.

Irradiated cells that contained AuNR-PEG (+AuNR) experienced in some cases pronounced increases of temperature (Figure 3), which severely impaired their viability after irradiation (Figure 4). High temperatures impaired mitochondrial activity, reducing the viability of the cell lines drastically, occasionally down to 50% immediately after treatment. This initial drop in cellular viability could be observed in all cell lines except for the Hek293 cell line, for which, even after 24 h, the mild increase of temperature experienced (maximum of 42 °C) did not seem to impair the mitochondria. All noncancerous cell lines had higher viabilities after irradiation compared to their diseased counterparts (Figure S5). In the case of kidney cell lines, these differences between cancer and noncancer cell lines were very pronounced, with the 786-0 cell line much less viable than the Hek293 cell line. This difference could be explained by the different temperatures reached during irradiation. However, large changes in temperature were also recorded for lung and hepatic cells, but in this case differences in viability were much less pronounced. Both lung cell lines seemed to recover some mitochondrial activity at 24 h after irradiation, and the differences found immediately after treatment faded after 24 h. In contrast, the hepatic cell lines had very similar viabilities immediately after treatment, but after 24 h significant differences were found after a drop in viability of HepG2 cells.

We also studied cell viability with Trypan Blue staining (Figure 5). For cancer cell lines with AuNR-PEG, the increase of temperature had an impact on membrane integrity. All three cell lines had lower viabilities at 24 h after irradiation than immediately after treatment (Figure 5A–C), although this decline of viability was only significant for 786-0 cells. On the other hand, A549 cells appeared to have a membrane that is more resistant to hyperthermia and laser irradiation, with a viability over 90% (Figure 5B).

In the case of noncancerous cell lines, no differences were found between the different conditions (CTL, øAuNR, +AuNR) at any time point after treatment (Figure 5G). Hek293 cells showed high resistance to either light or light + AuNR-PEG immediately and after 24 h, while NL20 cells seemed to be more affected by the increase of temperature. On the other hand, THLE-3 cells lost membrane integrity from the application of light alone, and this impairment increased with the presence of AuNR-PEG.

https://doi.org/10.1021/acsnanoscienceau.2c00023
ACS Nanosci. Au 2022, 2, 494–502

When comparing cell types irradiated with AuNR-PEG, 786-0 and Hek293 cells reach the highest temperatures when compared to cancerous and noncancerous cell lines, respectively; however, they showed opposite responses. The 786-0 cells were less viable than A549 and HepG2 cells, although the differences were not statistically significant (Figure S6). However, Hek293 cells had a statistically significant higher resistance to hyperthermia compared with NL20 and THLE-3 cells. This seemingly higher thermotolerance of low hyperthermia of Hek293 cells could be an adaptive response of the embryologic nature of this cell line. In any case, at 24 h after irradiation, viabilities for noncancerous cell lines with AuNR-PEG were higher than those of their diseased counterparts.

Our results indicated that increases of temperature favored an apoptotic cell death mechanism (loss of mitochondrial function) over a necrotic one (membrane rupture) with low power density irradiation. Other studies showed how high temperatures achieved with higher laser powers favor the induction of necrosis,[28] although apoptosis can be triggered with the combination of different types of nanoparticles and laser irradiation.[40−47] Under the laser conditions used, we can confirm that the laser irradiation settings employed are nontoxic for these cell lines *in vitro* but, in cells with AuNR-PEG, maximum temperature, mitochondrial activity and membrane integrity differed between cell types. Our findings are in good agreement with the use of low AuNR concentration, laser power, and exposure time to promote apoptosis.[44]

Correlations

Studying the variables of PPTT in parallel can be used to observe associations between them. Nanoparticle toxicity together with cellular uptake can provide a lot of information regarding cellular resistance to nanoparticles and their materials. Bhamidipati and Fabris[36] studied the correlation of uptake of AuNRs, gold nanostars, and gold nanospheres in U87 cells (human glioblastoma) and fibroblasts, but no correlation could be established between the two factors for the values reported. Our results, in disagreement with the outcomes of Bhamidipati, found a negative correlation between the number of nanoparticles incorporated and cytotoxicity ($r = -0.83$). The higher uptake by cells was in agreement with a decrease of cellular viability when studied with the MTT assay, the gold standard assay for cytotoxicity.[37] Discrepancies between studies highlight the importance of studying cytotoxicity for different cell types, tissues, and nanoparticles individually, almost erasing the possibility of extrapolating results.

Cellular uptake will also impact the temperatures reached during irradiation. Although this correlation will be prone to fluctuations depending on the laser setup, with the settings used throughout our research (3 W/cm^2, 3 min, 808 nm), a positive correlation was established between the number of AuNR-PEG incorporated and temperature ($r = 0.85$). Additionally, cell size and exocytosis rate also have a role on cellular uptake and photothermal heating.[45] Different cell sizes denote different cell volumes, which influences the location and distribution of internalized nanoparticles. Two cell lines may have a similar number of internalized nanoparticles when the metrics used are nanoparticle/cell; however, a larger cell will have a greater dispersion of nanoparticles inside the cell, affecting the collective thermal effects and intracellular heat dissipation. This is a limitation of the dose metrics typically used to express uptake and is a factor to consider during results extrapolation and standardization. Moreover, different cell sizes affect the biocompatibility of the material due to changes in mass concentration inside the cell.

Increases of temperature should be inversely correlated with viability. Both immediately and at 24 h after treatment, high temperatures correlated to a decrease in viability as studied by mitochondrial activity. Although the correlation coefficients are similar between the two time points ($r = -0.68$ and $r = -0.65$), a trending line emphasizes a more pronounced decrease of viability 24 h after irradiation (Figure S7). As previously mentioned, this further decrease of viability might be the result of a dynamic cell death process, instead of a single event. Loss of membrane integrity shows slightly different results compared to mitochondrial activity, as immediately after irradiation high temperatures do not strongly correlate with loss of viability ($r = -0.50$). However, this trend changes after 24 h ($r = -0.75$), indicating that the effects of temperature on cell lines are not immediate and the study of viability at two different time points, with different methods, is recommended. The approaches selected should look at different markers of viability: metabolic activity (e.g., MTT, XTT), membrane permeability (e.g., Trypan Blue or propidium iodide staining), enzymatic activity (e.g., LDH), or DNA synthesis/replication.[46]

CONCLUSIONS AND OUTLOOK

Currently, there is a remarkable imbalance between the large number of preclinical studies on photothermal therapy and the few clinical trials conducted to date. There are multiple and varied factors underlying this disproportion, from nanoparticle-related issues to technical hurdles of the treatment itself.[3] At this stage of maturity of PPTT, animal experimentation is unavoidable, but *in vitro* models play a key role in the reduction and refinement of the number of animals required. Identifying potential obstacles at the *in vitro* level of development, such as toxicity to nontarget organs either from the nanomaterial or from light treatment, allows for changes and refinement of the technique without the need for large cohorts of animals. The current work highlights the differences in cellular uptake, toxicity, and viability after treatment with PPTT for different cell types and tissues while maintaining the parameter space constant through the experiment.

As seen in this paper, differential uptake and sensitivity to the nanomaterial translate to cell type susceptibility in PPTT. Hence, *in vitro* experiments should be thoroughly designed to produce robust and reliable data to set a solid basis for further *in vivo* experiments. Using more complex *in vitro* systems, like cocultures and 3D cell culture methods, can give key information on communication between neighboring cell types and help unravel the different behaviors cells can show in PPTT. Moreover, the combination of such cellular systems with lab-on-a-chip technologies would provide PPTT research with a powerful tool for high throughput analysis, where many variables and outcomes can be tested in a more realistic tumor environment, allowing for a better understanding of all biological process involved in PPTT, from nanomaterial uptake to cell death mechanisms. Altogether, improving and standardizing *in vitro* studies will undoubtedly direct *in vivo* studies, which will, in turn, produce more quality preclinical data, ultimately favoring the clinical translation of PPTT.

https://doi.org/10.1021/acsnanoscienceau.2c00023
ACS Nanosci. Au 2022, 2, 494−502

METHODS

AuNR Synthesis and Surface Functionalization

AuNRs of 11 × 44 nm^2 were synthesized in-house using a modified seed-method[47−49] in a cetyltrimethylammonium bromide (CTAB) suspension. Suspensions were surface modified with polyethylene glycol (PEG) to remove toxic CTAB chains. Further details on synthesis, surface modification, and optical measurements are described in the Supporting Information (SI).

Cell Type and Sample Preparation

The 786-0 (human renal adenocarcinoma), A549 (human lung carcinoma), HepG2 (human liver carcinoma), Hek293 (human nontumorigenic embryo kidney), NL20 (immortalised human nontumorigenic lung), and THLE-3 (immortalised human nontumorigenic liver) cell lines were obtained from ATCC and cultured as specified by manufacturer's recommendations at 37 °C in a 5% CO_2 humidified environment. Further information on cell lines is described in the SI.

For uptake quantification of AuNR-PEG, 5000 cells were seeded in 96-well plates (polystyrene clear flat bottom, ThermoFisher Scientific) and allowed to grow for 2 days. For cytotoxicity assays, 2×10^4 cells were seeded in 24-well plates (polystyrene clear flat bottom, Nunc Microwell, ThermoFisher Scientific) and allowed to grow for 3 days. For photothermal irradiation, 2×10^5 cells were seeded in 6-well plates (polystyrene clear flat bottom, Nunc Microwell, ThermoFisher Scientific) and allowed to multiply until each well contained 8×10^5 cells.

Prior to incubation with AuNR-PEG, wells were washed with appropriate culture medium without supplements and AuNR-PEG were added, diluted in culture medium without FBS for cancer cell lines and with 5−10% FBS for healthy cell lines, at the concentrations specified for each experiment.

In Vitro Quantification of AuNR-PEG Uptake

Two-photon luminescence (TPL) images for *in vitro* quantification of AuNR-PEG were acquired using a confocal microscope (Leica TCS SP5, Leica Mycrosystems) coupled to a Kerr lens mode-locked Ti:sapphire laser with a 200 fs pulse duration (Mira900, Coherent) tuned at the absorption peak of the AuNR-PEG (focused around 810 nm).

AuNR-PEG were incubated for all cell lines at four different molar concentrations (0, 1, 2, and 5 nM) for 24 h. Before imaging, excess AuNR-PEG was removed and wells were washed twice in phosphate-buffered saline (PBS). Cells were fixed with 4% paraformaldehyde (PFA) in PBS. Further information on analysis is described at the SI.

In Vitro Determination of AuNR-PEG Toxicity

AuNR-PEG cytotoxicity was analyzed at six different molar concentrations (0, 1, 2, 4, 6, and 8 nM) after 24 h of incubation by adding thiazolyl blue tetrazolium bromide (MTT, M2128, CAS 298-93-1, Sigma-Aldrich) to a final concentration of 0.5 mg/mL. Plates were incubated at 37 °C for 30 min. The MTT solution was then removed, and formazan crystals were dissolved in 300 μL of dimethyl sulfoxide (DMSO, D8418, Sigma-Aldrich). Plates were read at 550 and 750 nm on a microplate reader (Synergy H1, BioTek Instruments). Every cell line had appropriate alive controls (0 nM) and four replicas per condition. Viability was calculated as percent of the alive control group.

Photothermal Irradiation (PPTT)

A suspension of 8×10^5 cells in 20 μL on a 96-well plate (Round bottom, Corning 3879, Corning Inc.) was irradiated from the top with a 3 mm diameter cw collimated laser beam from a Ti:sapphire laser (LU0808D 180 diode laser, LuOcean Mini, Lumics GmbH) adjusted to a wavelength of 808 nm. A single laser power (3 W/cm^2) and time of irradiation (3 min) were used throughout all the cell lines. This setting was selected after evaluating the effect different powers and time of irradiation had on cellular viability on 786-0 cells (Table S1).

Temperature was recorded continuously using an infrared camera (A35sc, FLIR Systems) at 30 Hz in a region that covered the diameter of the laser beam and sample. The temperature of the well plate was controlled with an autoregulated thermal bed (Homeothermic monitoring system, Harvard Apparatus) to maintain constant starting temperatures. In the irradiated wells, temperature was recorded 10 s prior illumination and 120 s after irradiation.

After irradiation, viability was evaluated at two different time points, immediately (TAT 0h) and 24 h after treatment (TAT 24h). After illumination, the cell suspension was recovered in 1 mL of appropriate cell culture medium without FBS and 500 μL of the sample was used to examine viability immediately after treatment (TAT 0h). Two complementary cell viability assays were used to analyze cells: trypan blue (TB) staining and MTT assay. For TB staining analysis, 50 μL of the sample was stained with 12.5 μL of TB solution (0.4%, Gibco, ThermoFisher Scientific) and placed in a hemocytometer for cell counting. For MTT assay, 50 μL of MTT 5 mg/mL was added to the remaining 450 μL of cell suspension and incubated 30 min at 37 °C. After incubation, samples were centrifuged, 90% of the supernatant removed, and 1 mL of DMSO was added to read samples as described above.

The remaining 500 μL from the initial suspension was reseeded in a 6-well plate with 1 mL of complete cell culture media and allowed to rest overnight at 37 °C in a 5% CO_2 incubator. At 24 h after treatment (TAT 24h), the cell culture medium and attached cells were recovered from each well and centrifuged to pellet the cells. Next, the cells were resuspended in 500 μL of appropriate culture medium without FBS. The same protocol followed for TAT 0h was followed for samples at TAT 24h.

Viability was calculated as percent of the alive control group (without AuNR-PEG and not irradiated) for the MTT analysis. In the case of TB, results are percent of death and alive cells in each condition.

ASSOCIATED CONTENT

Supporting Information

The Supporting Information is available free of charge at https://pubs.acs.org/doi/10.1021/acsnanoscienceau.2c00023.

Gold nanorod synthesis and PEG functionalization; *in vitro* quantification of AuNR-PEG uptake; statistics and figure design; representative images of bright field and two-photon luminescence from *in vitro* uptake; temperature and viability of irradiated 786-0 cell line at different laser powers and times of irradiation; absolute increases of temperature for irradiated cells without AuNR-PEG; correlation plots; rearranged data from Figures 1, 2, 4, and 5 for ease of comparison (PDF)

AUTHOR INFORMATION

Corresponding Authors

Clara Vilches − *ICFO − Institut de Ciències Fotòniques, the Barcelona Institute of Science and Technology, 08860 Castelldefels (Barcelona), Spain;* orcid.org/0000-0002-2695-2128; Email: clara.vilches@icfo.eu

Romain Quidant − *Nanophotonic Systems Laboratory, Department of Mechanical and Process Engineering, ETH Zürich, 8092 Zürich, Switzerland; ICFO − Institut de Ciències Fotòniques, the Barcelona Institute of Science and Technology, 08860 Castelldefels (Barcelona), Spain; ICREA − Institució Catalana de Recerca i Estudis Avançats, 08010 Barcelona, Spain;* orcid.org/0000-0001-8995-8976; Email: rquidant@ethz.ch

Author

Helena Villuendas − *Nanophotonic Systems Laboratory, Department of Mechanical and Process Engineering, ETH Zürich, 8092 Zürich, Switzerland; ICFO − Institut de*

Ciències Fotòniques, the Barcelona Institute of Science and Technology, 08860 Castelldefels (Barcelona), Spain;
orcid.org/0000-0002-7972-1892

Complete contact information is available at:
https://pubs.acs.org/10.1021/acsnanoscienceau.2c00023

Author Contributions

H.V. designed and performed the experiments, measured the data, and wrote the manuscript. C.V. designed and reviewed the experiments and contributed to writing the manuscript. R.Q. supervised and managed the study. CRediT: **Helena Villuendas** data curation (lead), formal analysis (lead), investigation (equal), methodology (equal), writing-original draft (lead), writing-review & editing (equal); **Clara Vilches** formal analysis (supporting), investigation (equal), methodology (equal), supervision (lead), writing-original draft (equal), writing-review & editing (equal); **Romain Quidant** conceptualization (lead), formal analysis (supporting), funding acquisition (lead), project administration (lead), writing-original draft (equal), writing-review & editing (equal).

Notes

The authors declare no competing financial interest.

■ ACKNOWLEDGMENTS

The authors acknowledge financial support from Fundació Privada CELLEX, the CERCA programme, and the Spanish Ministry of Economy and Competitiveness, through the "Severo Ochoa" Programme for Centres of Excellence in R&D (SEV-2015-0522). H.V. acknowledges financial support from fellowship program Severo Ochoa-MINECO 2018 (SEV-2015-0522-18-3). The authors would like to thank Dr. Ignacio de Miguel for technical support and Dr. Jaime Ortega Arroyo for fruitful discussions.

■ ABBREVIATIONS

PPTT, plasmonic photothermal therapy; AuNR-PEG, gold nanorods; TPL, two-photon luminescence

■ REFERENCES

(1) Habash, R. W. Y. *Therapeutic hyperthermia, in Handbook of Clinical Neurology*, 1st ed.; Elsevier B.V., 2018; Vol. *157*, pp 853−868. DOI: 10.1016/B978-0-444-64074-1.00053-7.
(2) Bettaieb, A.; Wrzal, P. K.; Averill-bates, D. A. Hyperthermia: Cancer Treatment and Beyond. *Cancer Treat. Innov. Approaches* **2013**, 257−283.
(3) Vilches, C.; Quidant, R. Targeted hyperthermia with plasmonic nanoparticles. In *Frontiers of Nanoscience*, 1st ed.; Elsevier Ltd, 2020; Vol. *16*, pp 307−352. DOI: 10.1016/B978-0-08-102828-5.00012-7.
(4) Habash, R. W. Y.; Krewski, D.; Bansal, R.; Alhafid, H. T. Principles, applications, risks and benefits of therapeutic hyperthermia. *Front. Biosci.* **2011**, *E3* (June), 1169−1181.
(5) Norouzi, H.; Khoshgard, K.; Akbarzadeh, F. In vitro outlook of gold nanoparticles in photo-thermal therapy: a literature review. *Lasers Med. Sci.* **2018**, *33*, 917−926.
(6) Mooney, R.; Roma, L.; Zhao, D.; Van Haute, D.; Garcia, E.; Kim, S. U.; Annala, A. J.; Aboody, K. S.; Berlin, J. M. Neural Stem Cell-Mediated Delivery of Gold Nanorods Improves Intratumoral Photothermal Therapy. *ACS Nano* **2014**, *8*, 12450−12460.
(7) Beik, J.; Abed, Z.; Ghoreishi, F. S.; Hosseini-Nami, S.; Mehrzadi, S.; Shakeri-Zadeh, A.; Kamrava, S. K. Nanotechnology in hyperthermia cancer therapy: From fundamental principles to advanced applications. *J. Controlled Release* **2016**, *235*, 205−221.
(8) Riley, R. S.; Day, E. S. Gold nanoparticle-mediated photothermal therapy: applications and opportunities for multimodal cancer treatment. *Wiley Interdiscip. Rev.: Nanomed. Nanobiotechnol.* **2017**, *9*, 1−16.
(9) Abadeer, N. S.; Murphy, C. J. Recent Progress in Cancer Thermal Therapy Using Gold Nanoparticles. *J. Phys. Chem. C* **2016**, *120*, 4691−4716.
(10) Pattani, V. P.; Shah, J.; Atalis, A.; Sharma, A.; Tunnell, J. W. Role of apoptosis and necrosis in cell death induced by nanoparticle-mediated photothermal therapy. *J. Nanoparticle Res.* **2015**, *17*, 1−11.
(11) Huang, X.; El-Sayed, M. A. Gold nanoparticles: Optical properties and implementations in cancer diagnosis and photothermal therapy. *J. Adv. Res.* **2010**, *1*, 13−28.
(12) Huang, X.; El-Sayed, M. A. Plasmonic photo-thermal therapy (PPTT). *Alexandria J. Med.* **2011**, *47*, 1−9.
(13) de Melo-Diogo, D.; Pais-Silva, C.; Dias, D. R.; Moreira, A. F.; Correia, I. J. Strategies to Improve Cancer Photothermal Therapy Mediated by Nanomaterials. *Adv. Healthcare Mater.* **2017**, *6*, 1700073.
(14) Jaque, D.; Martínez Maestro, L.; del Rosal, B.; Haro-Gonzalez, P.; Benayas, A.; Plaza, J. L.; Martín Rodríguez, E.; García Solé, J. Nanoparticles for photothermal therapies. *Nanoscale* **2014**, *6*, 9494−9530.
(15) Bucharskaya, A. B.; Maslyakova, G. N.; Dikht, N. I.; Navolokin, N. A.; Terentyuk, G. S.; Bashkatov, A. N.; Genina, E. A.; Khlebtsov, B. N.; Khlebtsov, N. G.; Tuchin, V. V. Plasmonic Photothermal Therapy of Transplanted Tumors in Rats at Multiple Intravenous Injection of Gold Nanorods. *Bionanoscience* **2017**, *7*, 216−221.
(16) Sharifi, M.; Attar, F.; Saboury, A. A.; Akhtari, K.; Hooshmand, N.; Hasan, A.; El-Sayed, M. A.; Falahati, M. Plasmonic gold nanoparticles: Optical manipulation, imaging, drug delivery and therapy. *J. Controlled Release* **2019**, *311−312*, 170−189.
(17) Carnovale, C.; Bryant, G.; Shukla, R.; Bansal, V. Identifying Trends in Gold Nanoparticle Toxicity and Uptake: Size, Shape, Capping Ligand, and Biological Corona. *ACS Omega* **2019**, *4*, 242−256.
(18) Park, M. V. D. Z.; Lankveld, D. P. K.; van Loveren, H.; de Jong, W. H. The status of in vitro toxicity studies in the risk assessment of nanomaterials. *Nanomedicine* **2009**, *4*, 669−685.
(19) Xavier, M.; Parente, I. A.; Rodrigues, P. M.; Cerqueira, M. A.; Pastrana, L.; Gonçalves, C. Safety and fate of nanomaterials in food: The role of in vitro tests. *Trends Food Sci. Technol.* **2021**, *109*, 593−607.
(20) Guggenheim, E. J.; Milani, S.; Röttgermann, P. J. F.; Dusinska, M.; Saout, C.; Salvati, A.; Rädler, J. O.; Lynch, I. Refining in vitro models for nanomaterial exposure to cells and tissues. *NanoImpact* **2018**, *10*, 121−142.
(21) Morales-Dalmau, J.; Vilches, C.; De Miguel, I.; Sanz, V.; Quidant, R. Optimum morphology of gold nanorods for light-induced hyperthermia. *Nanoscale* **2018**, *10*, 2632−2638.
(22) Zhao, P.; Chen, X.; Wang, Q.; Zou, H.; Xie, Y.; Liu, H.; Zhou, Y.; Liu, P.; Dai, H. Differential toxicity mechanism of gold nanoparticles in HK-2 renal proximal tubular cells and 786−0 carcinoma cells. *Nanomedicine* **2020**, *15*, 1079−1096.
(23) Xia, Q.; Huang, J.; Feng, Q.; Chen, X.; Liu, X.; Li, X.; Zhang, T.; Xiao, S.; Li, H.; Zhong, Z.; Xiao, K. Size- and cell type-dependent cellular uptake, cytotoxicity and in vivo distribution of gold nanoparticles. *Int. J. Nanomedicine* **2019**, *14*, 6957−6970.
(24) Naha, P. C.; Chhour, P.; Cormode, D. P. Systematic in vitro toxicological screening of gold nanoparticles designed for nanomedicine applications. *Toxicol. Vitr.* **2015**, *29*, 1445−1453.
(25) Claudia, M.; Kristin, Ö.; Jennifer, O.; Eva, R.; Eleonore, F. Comparison of fluorescence-based methods to determine nanoparticle uptake by phagocytes and non-phagocytic cells in vitro. *Toxicology* **2017**, *378*, 25−36.
(26) Soenen, S. J.; Manshian, B. B.; Abdelmonem, A. M.; Montenegro, J. M.; Tan, S.; Balcaen, L.; Vanhaecke, F.; Brisson, A. R.; Parak, W. J.; De Smedt, S. C.; Braeckmans, K. The cellular interactions of PEGylated gold nanoparticles: Effect of PEGylation on cellular uptake and cytotoxicity. *Part. Part. Syst. Charact.* **2014**, *31*, 794−800.

(27) Almada, M.; Leal-Martínez, B. H.; Hassan, N.; Kogan, M. J.; Burboa, M. G.; Topete, A.; Valdez, M. A.; Juárez, J. Photothermal conversion efficiency and cytotoxic effect of gold nanorods stabilized with chitosan, alginate and poly(vinyl alcohol). *Mater. Sci. Eng., C* **2017**, *77*, 583−593.
(28) Zhang, Y.; Zhan, X.; Xiong, J.; Peng, S.; Huang, W.; Joshi, R.; Cai, Y.; Liu, Y.; Li, R.; Yuan, K.; Zhou, N.; Min, W. Temperature-dependent cell death patterns induced by functionalized gold nanoparticle photothermal therapy in melanoma cells. *Sci. Rep.* **2018**, *8*, 8720.
(29) Amaral, M.; Charmier, A. J.; Afonso, R. A.; Catarino, J.; Faísca, P.; Carvalho, L.; Ascensão, L.; Coelho, J. M. P.; Manuela Gaspar, M.; Reis, C. P. Gold-based nanoplataform for the treatment of anaplastic thyroid carcinoma: A step forward. *Cancers (Basel)* **2021**, *13*, 1242.
(30) Pérez-Hernández, M.; Del Pino, P.; Mitchell, S. G.; Moros, M.; Stepien, G.; Pelaz, B.; Parak, W. J.; Gálvez, E. M.; Pardo, J.; De La Fuente, J. M. Dissecting the molecular mechanism of apoptosis during photothermal therapy using gold nanoprisms. *ACS Nano* **2015**, *9*, 52−61.
(31) Mocan, T.; Matea, C. T.; Cojocaru, I.; Ilie, I.; Tabaran, F. A.; Zaharie, F.; Iancu, C.; Bartos, D.; Mocan, L. Photothermal treatment of human pancreatic cancer using PEGylated multi-walled carbon nanotubes induces apoptosis by triggering mitochondrial membrane depolarization mechanism. *J. Cancer* **2014**, *5*, 679−688.
(32) Fröhlich, E. The role of surface charge in cellular uptake and cytotoxicity of medical nanoparticles. *Int. J. Nanomedicine* **2012**, *7*, 5577−5591.
(33) Kim, J.; Chun, S. H.; Amornkitbamrung, L.; Song, C.; Yuk, J. S.; et al. Gold nanoparticle clusters for the investigation of therapeutic efficiency against prostate cancer under near - infrared irradiation. *Nano Convergence* **2020**, *7*, 1−9.
(34) Mohtar, N.; Parumasivam, T.; Gazzali, A. M.; Tan, C. S.; Tan, M. L.; Othman, R.; Fazalul Rahiman, S. S.; Wahab, H. A. Advanced Nanoparticle-Based Drug Delivery Systems and Their Cellular Evaluation for Non-Small Cell Lung Cancer Treatment. *Cancers (Basel)*. **2021**, *13*, 3539.
(35) Wilhelm, S.; Tavares, A. J.; Dai, Q.; Ohta, S.; Audet, J.; Dvorak, H. F.; Chan, W. C. W.; Chatterley, A.; W. Group. Analysis of Nanopar.cle Delivery to Tumours. *Nat. Rev. Mater.* **2016**, *1*, 16014.
(36) Bhamidipati, M.; Fabris, L. Multiparametric Assessment of Gold Nanoparticle Cytotoxicity in Cancerous and Healthy Cells: The Role of Size, Shape, and Surface Chemistry. *Bioconjugate Chem.* **2017**, *28*, 449−460.
(37) Alkilany, A. M.; Murphy, C. J. Toxicity and cellular uptake of gold nanoparticles: What we have learned so far? *J. Nanoparticle Res.* **2010**, *12*, 2313−2333.
(38) Baffou, G.; Berto, P.; Bermúdez Ureña, E.; Quidant, R.; Monneret, S.; Polleux, J.; Rigneault, H. Photoinduced heating of nanoparticle arrays. *ACS Nano* **2013**, *7*, 6478−6488.
(39) Qi, G.; Zhang, Y.; Xu, S.; Li, C.; Wang, D.; Li, H.; Jin, Y. Nucleus and Mitochondria Targeting Theranostic Plasmonic Surface-Enhanced Raman Spectroscopy Nanoprobes as a Means for Revealing Molecular Stress Response Differences in Hyperthermia Cell Death between Cancerous and Normal Cells. *Anal. Chem.* **2018**, *90*, 13356−13364.
(40) Guerrero-Florez, V.; Mendez-Sanchez, S. C.; Patrón-Soberano, O. A.; Rodríguez-González, V.; Blach, D.; Fernando Martínez, O. Gold nanoparticle-mediated generation of reactive oxygen species during plasmonic photothermal therapy: a comparative study for different particle sizes, shapes, and surface conjugations. *J. Mater. Chem. B* **2020**, *8*, 2862−2875.
(41) Liu, Y.; Yang, M.; Zhang, J.; Zhi, X.; Li, C.; Zhang, C.; Pan, F.; Wang, K.; Yang, Y.; Martinez De La Fuentea, J.; Cui, D. Human Induced Pluripotent Stem Cells for Tumor Targeted Delivery of Gold Nanorods and Enhanced Photothermal Therapy. *ACS Nano* **2016**, *10*, 2375−2385.
(42) Wu, Y.; Ali, M. R. K.; Dong, B.; Han, T.; Chen, K.; Chen, J.; Tang, Y.; Fang, N.; Wang, F.; El-Sayed, M. A. Gold Nanorod-Photothermal Therapy Alters Cell Junctions and Actin Network in Inhibiting Cancer Cell Collective Migration. *ACS Nano* **2018**, *12*, 9279−9290.
(43) Liu, Y.; Xu, M.; Zhao, Y.; Chen, X.; Zhu, X.; Wei, C.; Zhao, S.; Liu, J.; Qin, X. Flower-like gold nanoparticles for enhanced photothermal anticancer therapy by the delivery of pooled siRNA to inhibit heat shock stress. *J. Mater. Chem. B* **2019**, *7*, 586−597.
(44) Ali, M. R. K.; Wu, Y.; El-Sayed, M. A. Gold Nanoparticle-Assisted Plasmonic Photothermal Therapy Advances Towards Clinical Application. *J. Phys. Chem. C* **2019**, *123*, No. 15375.
(45) Sun, X.; Gamal, M.; Nold, P.; Said, A.; Chakraborty, I.; Pelaz, B.; Schmied, F.; von Pückler, K.; Figiel, J.; Zhao, Y.; Brendel, C.; Hassan, M.; Parak, W. J.; Feliu, N. Tracking stem cells and macrophages with gold and iron oxide nanoparticles − The choice of the best suited particles. *Appl. Mater. Today* **2019**, *15*, 267−279.
(46) Ramos, T. I.; Villacis-Aguirre, C. A.; López-Aguilar, K. V.; Padilla, L. S.; Altamirano, C.; Toledo, J. R.; Vispo, N. S. The Hitchhiker's Guide to Human Therapeutic Nanoparticle Development. *Pharmaceutics* **2022**, *14*, 247.
(47) Pérez-Juste, J.; Pastoriza-Santos, I.; Liz-Marzán, L. M.; Mulvaney, P. Gold nanorods: Synthesis, characterization and applications. *Coord. Chem. Rev.* **2005**, *249*, 1870−1901.
(48) Nikoobakht, B.; El-Sayed, M. A. Preparation and growth mechanism of gold nanorods (NRs) using seed-mediated growth method. *Chem. Mater.* **2003**, *15*, 1957−1962.
(49) Morales-Dalmau, J.; Vilches, C.; Sanz, V.; de Miguel, I.; Rodríguez-Fajardo, V.; Berto, P.; Martínez-Lozano, M.; Casanovas, O.; Durduran, T.; Quidant, R. Quantification of gold nanoparticle accumulation in tissue by two-photon luminescence microscopy. *Nanoscale* **2019**, *11*, 11331−11339.

https://doi.org/10.1021/acsnanoscienceau.2c00023
ACS Nanosci. Au 2022, 2, 494−502